



Forcing oscillatory media: phase kinks vs. synchronization

Hugues Chaté^a, Arkady Pikovsky^{b,*}, Oliver Rudzick^b

^a CEA – Service de Physique de l’Etat Condensé, Centre d’Etudes de Saclay, 91191 Gif-sur-Yvette, France

^b Department of Physics, University of Potsdam, Am Neuen Palais, PF 601553, D-14415, Potsdam, Germany

Abstract

We consider the effect of periodic external forcing on the spatiotemporal dynamics of one-dimensional oscillatory media modelled by the complex Ginzburg–Landau equation (CGLE). We determine the domain of existence and linear stability of the spatially homogeneous synchronous solution found at strong forcing. Some of the synchronization scenarios observed are described, and the “turbulent synchronized states” encountered are detailed. We show that 2π -phase kinks are the ubiquitous objects mediating synchronization and study their nontrivial dynamics. In particular, we consider the processes of kink-breeding and the spontaneous creation of kinks which are specific to our phase and amplitude description. The general consequences, at the statistical level, of breaking the gauge invariance of the CGLE by a periodic forcing are discussed. ©1999 Elsevier Science B.V. All rights reserved.

Keywords: Phase-locking; Ginzburg–Landau equation; Phase turbulence; Amplitude turbulence; Spatiotemporal intermittency

1. Introduction

One of the basic features of periodic self-sustained oscillations is their sensitivity to external driving. Even a small external force can affect the dynamics, provided the frequency of the forcing is close to the natural frequency of the oscillator. The effect of frequency entrainment, known as synchronization since the pioneering work of Huygenii [1], is widely observed in natural systems [2]. Much less is known of spatially extended situations. In this paper, we consider the effect of a periodic external forcing on nonlinear oscillatory media.

The complex dynamics of spatially extended systems is, to a large extent, determined by the nature of the primary instability they undergo [3,4]. In many

cases, this instability is oscillatory: the unstable mode has a nonzero frequency. If the instability is supercritical, a general description of the oscillatory medium near the instability border is given by the complex Ginzburg–Landau equation (CGLE) [5]:

$$\partial_t a = (1 + i\omega_0)a - (1 + i\alpha)|a|^2 a + (1 + i\beta)\nabla^2 a, \quad (1)$$

where a is the complex amplitude of the oscillations, ω_0 is their natural (linear) frequency, and α and β are the two remaining real parameters after rescaling of time, space, and a . As is apparent in (1), the CGLE can be seen as a direct generalization of the amplitude equation for a local self-sustained (Hopf) oscillator to the case of spatially variable fields with diffusive coupling. It is thus a universal equation asymptotically exact near the instability border, but whose validity is now widely believed to extend far beyond the vicinity

* Corresponding author. Fax: +49 331 977 1142; e-mail: pikovsky@stat.physik.uni-postdam.de.

of the threshold (for recent experimental examples, see, e.g. [6,7]). The CGLE has attracted a large interest and is now quite well understood, at least in one and two space dimensions [8–14].

In this work, we study the effect of a periodic external forcing on an oscillatory medium described by the CGLE. We restrict ourselves to the one-dimensional case, for which the CGLE already exhibits a wide variety of dynamical regimes [9]. We consider a weak, nonparametric (additive) forcing, whose main effects are expected to manifest themselves when the forcing frequency is close to the natural frequency of the autonomous system. More general parametric forcings have been considered in [15,16], where the additive forcing case has also been briefly discussed; a case when the forcing term results from the mean field has been studied in [17]. We focus in particular on the properties of the 2π -phase kinks that appear in the forced medium. We show that these localized objects, characteristic of the broken gauge invariance ($a \rightarrow ae^{i\phi}$) of the forced CGLE, are the building blocks of new partially synchronized dynamical regimes.

The paper is organized as follows. In Sections 2 and 3, we recall briefly the basic properties of the CGLE, introduce forcing, and investigate the existence and stability of the spatially homogeneous solution in full synchrony with the external forcing. In Section 4, we present, using numerical simulations, the synchronization scenarios of phase- and defect-turbulence, two of the main dynamical regimes of the CGLE. The 2π -phase kinks are introduced in Section 5 as the natural excitations of forced oscillatory media. Their dynamics and its effect on the synchronization properties of the medium are described in Section 6. We conclude by listing problems worth further investigation, together with natural extensions and perspectives offered by the present work.

2. Basic model

2.1. Autonomous CGLE

In this section we briefly review the basic properties of the *autonomous* CGLE [4]. In (1), the linear

frequency ω_0 can be eliminated by a transformation to a rotating reference frame, so that only α and β (and, possibly, initial conditions) determine the dynamics, if we assume the system size L to be large enough so as to have negligible influence. An approximate phase diagram, showing the regions corresponding to different regimes in the (α, β) plane, was given in [9]. These regions are determined, to a large extent, by the stability properties of the family of plane wave solutions to the CGLE. These solutions read, in one dimension:

$$a = a_k \exp(ikx - i\omega_k t),$$

with

$$a_k^2 = 1 - k^2 \quad \text{and} \quad \omega_k = -\omega_0 + \alpha + (\beta - \alpha)k^2.$$

They are linearly stable if and only if

$$1 + \alpha\beta > 0 \quad \text{and} \quad k^2 < k_{\max}^2(\alpha, \beta). \quad (2)$$

When $1 + \alpha\beta < 0$, two kinds of disordered regimes are observed: *phase turbulence*, where no zeroes of a occur – and thus the phase $\phi \equiv \arg a$ is always defined¹ – and *defect turbulence* where a finite density of zeroes of a is recorded in space–time. In the region $1 + \alpha\beta > 0$, some plane wave solutions are stable, but they do not necessarily constitute a global attractor: sustained regimes of *spatiotemporal intermittency* exist, composed of patches of stable plane wave solutions separated by localized propagating objects.

The gauge invariance of the CGLE implies that the dynamics around the plane wave solutions may be effectively described by phase-only equations exploiting the marginality of the soft phase mode and the strong damping of amplitude ($R \equiv |a|$) modes. Near the $1 + \alpha\beta = 0$, and in particular for $1 + \alpha\beta > 0$, the instability of the plane wave solutions is weak, and the phase dynamics occurs on long scales in space and time, according to

$$\partial_t \phi = \omega_0 + (\alpha - \beta)\phi_x^2 + (1 + \alpha\beta)\phi_{xx},$$

¹To be comprehensive, it is actually believed that phase slips may still occur in the infinite-size, infinite-time, limit. However, the probability of these events is so small, in the usually delimited phase turbulence region, that they never occur in practice [11].

where subscripts denote partial derivatives. This equation is valid to second-order in the phase gradient, like the corresponding expression for the modulus:

$$R \approx 1 - \frac{\phi_x^2 + \beta\phi_{xx}}{2}.$$

2.2. Periodically forced CGLE

Adding an external harmonic forcing of amplitude B and frequency ω_e , and going to a frame rotating with this external forcing ($a \rightarrow A \equiv a \exp(-i\omega_e t)$), Eq. (1) reads, in one dimension:

$$\begin{aligned} \partial_t A = (1 + i\nu)A - (1 + i\alpha)|A|^2 A \\ + (1 + i\beta)A_{xx} + B, \end{aligned} \quad (3)$$

where $\nu = \omega_0 - \omega_e$ is the frequency mismatch between the frequency of the external force ω_e and the linear frequency ω_0 .²

Substituting $A = R e^{i\Phi}$, we get a system of two real equations for the modulus and the phase

$$\begin{aligned} \partial_t R = R - R^3 - \beta R \Phi_{xx} - 2\beta R_x \Phi_x - R(\Phi_x)^2 \\ + R_{xx} + B \cos \Phi, \\ R \partial_t \Phi = \nu R - \alpha R^3 + R \Phi_{xx} + 2R_x \Phi_x \\ - \beta R(\Phi_x)^2 + \beta R_{xx} - B \sin \Phi. \end{aligned} \quad (4)$$

Again, as in the case of the autonomous system, a phase equation can be approximately derived if, in addition, the parameters B and $\nu - \alpha$ are small [15,16]:

$$R \approx 1 - \frac{\phi_x^2 + \beta\phi_{xx} - B \cos \Phi}{2}, \quad (5)$$

$$\begin{aligned} \dot{\Phi} = \nu - \alpha - B \sin \Phi - B\alpha \cos \Phi + (\alpha - \beta)\Phi_x^2 \\ + (1 + \alpha\beta)\Phi_{xx}. \end{aligned} \quad (6)$$

²Note that we assume here that the frequency of the external force is close to the frequency of the free oscillations, and thus restrict ourselves to the resonance 1:1. Higher resonances can also be considered, and in this case terms of the type $B^m(A^*)^n$ appear on the right-hand side of Eq. (3), cf. [15,16]. For example, if the frequency of the forcing is close to $2\omega_0$, parametric resonance appears, described by the term $\sim BA^*$. If the amplitude of the oscillations and of the external force are small, higher-order resonances can be neglected compared to the main resonance 1:1 (the corresponding phase-locking regions – Arnold tongues – being very narrow).

3. The spatially homogeneous state and its stability

Spatially homogeneous solutions to the forced CGLE are obtained by setting all spatial derivatives to zero in (4). We get the system

$$\begin{aligned} \dot{R} = R - R^3 + B \cos \Phi, \\ R \dot{\Phi} = \nu - \alpha R^3 - B \sin \Phi. \end{aligned} \quad (7)$$

These equations, with a slightly different normalization, have been thoroughly studied in [18], where a rich bifurcation diagram was found. Here, we restrict our analysis to the case of a relatively small forcing, where the bifurcation structure is simple.

The fixed points are given by

$$\begin{aligned} R_0 - R_0^3 + B \cos \Phi_0 = 0, \\ \nu R_0 - \alpha R_0^3 - B \sin \Phi_0 = 0. \end{aligned} \quad (8)$$

Excluding the phase, we get

$$B^2 = R_0^2(1 - R_0^2)^2 + R_0^2(\nu - \alpha R_0^2)^2, \quad (9)$$

which has either 1 or 3 positive roots. In the latter case, two roots tend to 1 as $B \rightarrow 0$ and $\nu \rightarrow \alpha$, thus converging to the nontrivial solution of the autonomous CGLE. These two roots describe the two spatially homogeneous solutions in synchrony with the forcing. One is stable, the other unstable. The stable root corresponds to the phase-locking of a homogeneous oscillating solution of the autonomous CGLE. In full analogy with the problem of the synchronization of single oscillators, we call the region of existence of these two solutions the phase-locked region, or the Arnol'd tongue. The borders of the Arnol'd tongue can be determined from the condition that Eq. (9) has two coinciding real roots; this gives the relation

$$\begin{aligned} 27B_{\text{A.t.}}^4(1 + \alpha^2)^2 - B_{\text{A.t.}}^2(1 + \alpha\nu)(9(\nu - \alpha)^2 \\ + (1 + \alpha\nu)^2) + 4(1 + \nu^2)^2(\nu - \alpha)^2 = 0. \end{aligned}$$

To first order in $|\nu - \alpha|$, the borders of the Arnol'd tongue are given by

$$B_{\text{A.t.}}^2 = \frac{(\nu - \alpha)^2}{(1 + \alpha^2)}.$$

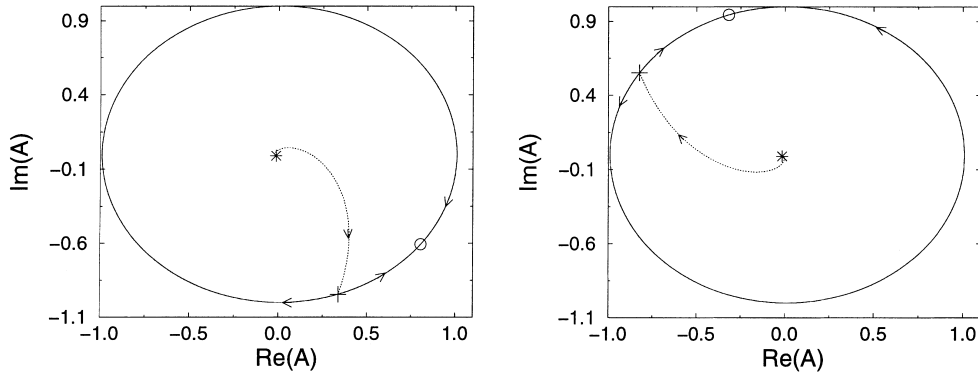


Fig. 1. Phase portraits of the ODE system (7): (a) $v = -0.0775$, $\alpha = -0.75$, and $B = 0.021$; (b) $v = -0.725$, $\alpha = -0.75$, and $B = 0.021$. Circle: the stable fixed point corresponding to a phase-locked solution, plus: an unstable saddle; star: an unstable focus.

The two synchronous solutions inside the Arnol'd tongue are a stable node and an unstable saddle (Fig. 1). Near the borders of the tongue, the saddle and the node approach each other, and the system is excitable: a small perturbation of the stable fixed point may lead to an excursion along the unstable manifold of the saddle, and a 2π -phase slip is observed. As we will see below, the asymmetry of the two borders of the Arnol'd tongue is important: writing $v = \alpha(1 + v')$, the excitation of the phase slip occurs for weaker perturbations for positive v' than for negative v' (this asymmetry disappears for $\alpha = 0$).

We now consider the stability of the synchronized spatially homogeneous solution with respect to spatially inhomogeneous perturbations. Setting

$$R = R_0 + r(x, t), \quad \Phi = \Phi_0 + \phi(x, t),$$

and linearizing system (4), we get

$$\begin{aligned} \partial_t r &= (1 - 3R_0^2)r + r_{xx} \\ &\quad - R_0(v - \alpha R_0^2)\phi - \beta R_0\phi_{xx}, \\ R_0\partial_t \phi &= (v - 3\alpha R_0^2)r + \beta r_{xx} \\ &\quad + R_0(1 - R_0^2)\phi + R_0\phi_{xx}. \end{aligned}$$

Solving for Fourier modes, we get the growth rate λ for the wave number k :

$$\lambda(k) = 1 - 2R_0^2 - k^2 \pm [R_0^4 - \alpha^2(1 - R_0^2)(1 - 3R_0^2) + 2\alpha\beta(1 - 2R_0^2)k^2 - \beta^2k^4]^{1/2}. \quad (10)$$

The location of the neutral curve $\max_k \lambda(k) = 0$ can be rewritten as

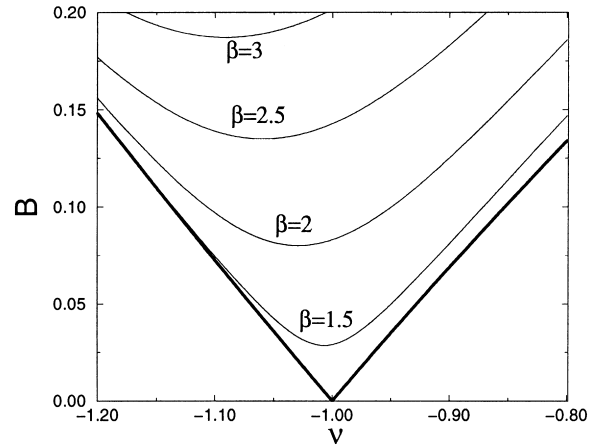


Fig. 2. The Arnol'd tongue (thick line) and the stability borders of homogeneous solution for $\alpha = -1$ and different values of β . The instability region disappears for $\alpha\beta = -1$.

$$R_0^4 [3(\alpha - \beta)^2 - (1 + \alpha\beta)^2] + 4R_0^2(\beta - \alpha)(v - \beta) + (\beta - v)^2 = 0. \quad (11)$$

In the $B = 0$ case, $v = \alpha$ and $R_0 = 1$, so this condition reduces to the Benjamin–Feir–Newell criterion (2). Otherwise, the spatially homogeneous field is stable if the amplitude exceeds the following critical value (see [19] for detailed analysis):

$$R_c^2 = \frac{(v - \beta)^2}{2(\alpha - \beta)(v - \beta) - |v - \beta|\sqrt{(1 + \alpha^2)(1 + \beta^2)}}. \quad (12)$$

Together with (9), this allows one to find the stability region inside the Arnol'd tongue, as illustrated in Fig. 2. For small forcing amplitudes B , $R_0^2 \approx 1$, and

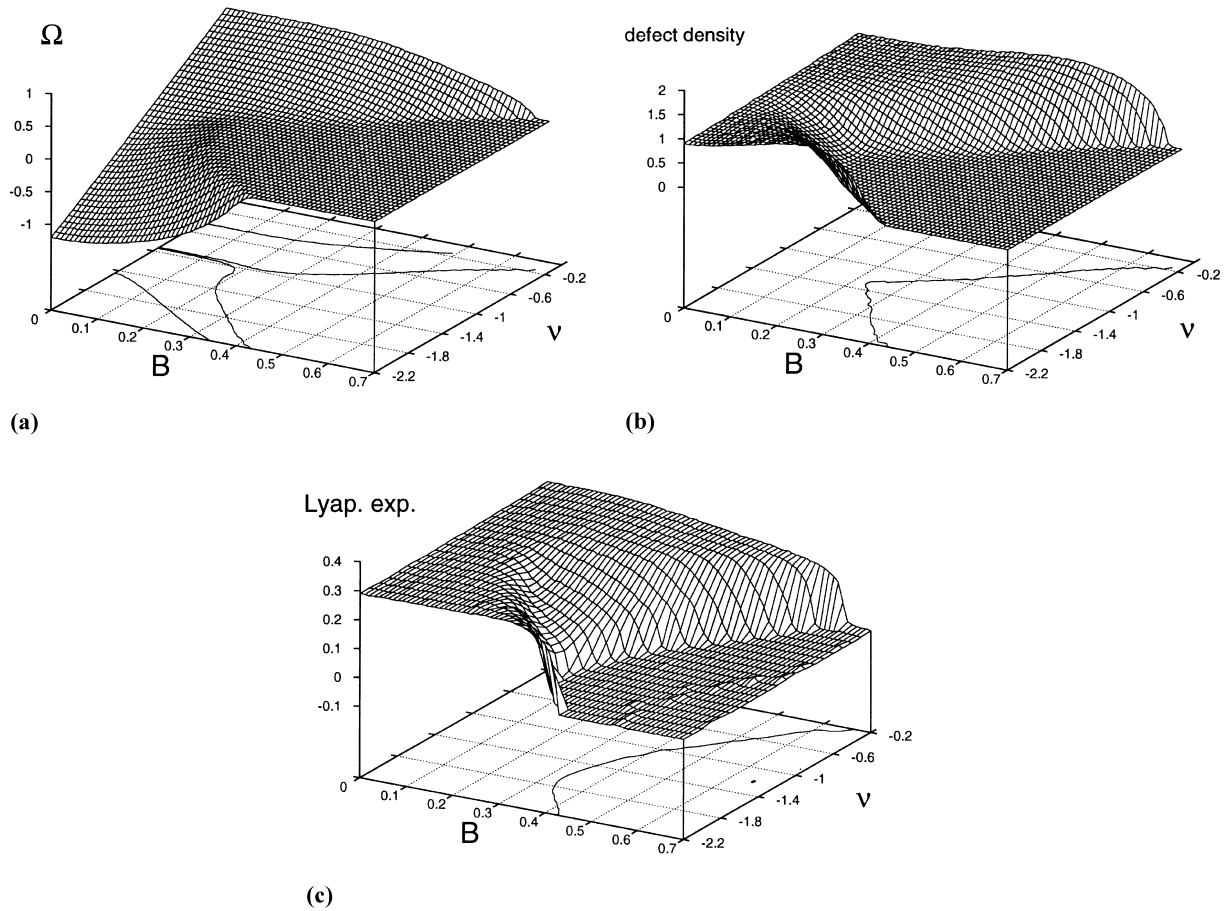


Fig. 3. Synchronization of defect turbulence: (a) Average frequency as a function of the amplitude B and the frequency ν of the external force. The contour lines are drawn at levels -0.5 , -0.01 , 0.01 , 0.5 . (b) Density of defects (arbitrary units). The contour line shows the border of the defect-free region. (c) The largest Lyapunov exponent. The contour line shows the border of the turbulent region.

thus, using (10), the growth rate λ is real at threshold with a finite wave number k . This stationary cellular instability, in the cases investigated numerically below, is always supercritical: beyond threshold, a stationary periodic structure is observed.

4. Global properties of synchronization

We now report on numerical investigations of the synchronization of turbulent states in the CGLE. Here, we are mostly concerned with the global synchronization properties of the regimes encountered when increasing the forcing of phase and defect turbulence.

In particular, we do not deal with the reverse scenario, where forcing is decreased from a fully synchronized state. Moreover, we do not attempt to describe all possible scenarios occurring in different ranges of parameters. We have chosen only two points on the (α, β) plane, namely $\alpha = -2$, $\beta = 2$ for defect turbulence, and $\alpha = -0.75$, $\beta = 2$ for phase turbulence. We have studied the different regimes observed at these parameter values for various values of the amplitude B and frequency ν of the external force. The results presented below are thus neither universal nor complete. We believe, however, that they are typical (i.e. that these or similar properties will be observed in large regions of parameter space).

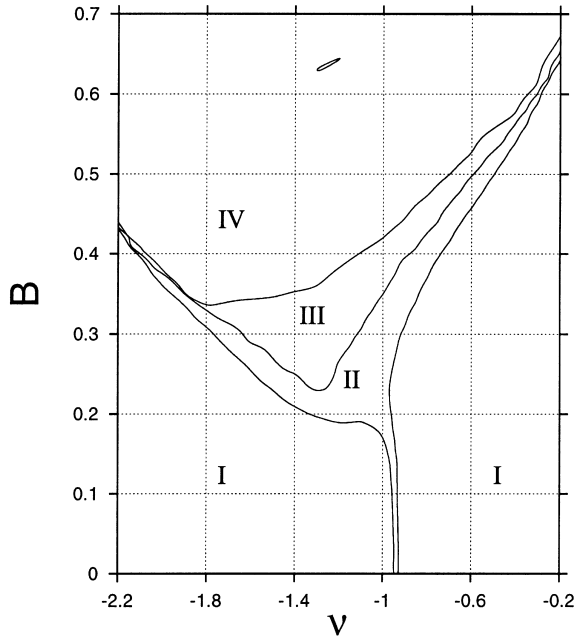


Fig. 4. Different regimes of synchronization of defect turbulence: (I) Defect turbulence, no synchronization. (II) Turbulent synchronization with rare defects. (III) Turbulent synchronization without defects. (IV) Regular state with zero Lyapunov exponent. The contour lines are drawn (from bottom to top) from the graphs of Fig. 3 at near-zero levels: for Ω at ± 0.002 , for the defect density at 2×10^{-4} , and for the Lyapunov exponent at 0.01. The levels deviate from zero because of the finite accuracy of calculations.

We have solved the forced CGLE (3) using a finite-difference method with the spatial step $\Delta x = 0.4$ and the time step $\Delta t = 0.025$. In all runs, we started from a turbulent nonforced state and increased the forcing amplitude in small steps. At each step, the statistically stationary regime has been analyzed after discarding transients, in particular, by measuring the average frequency of rotation $\Omega \equiv \langle \partial_t \Phi \rangle$, where the average is taken both in space and time (Ω is calculated in the reference frame rotating with the frequency of the external forcing, so the zero value of Ω corresponds to perfect synchronization). For the fully synchronous solution (8), $\partial_t \Phi = 0$ everywhere; but the average frequency Ω can also vanish for nontrivial spatiotemporal regimes, as shown below. We call such regimes, analogous to the phase synchronized regimes found in forced chaotic low-dimensional systems [20,21], “turbulent synchronized states”.

4.1. Synchronizing defect turbulence

The results of calculations of the average frequency Ω , of the density of defects, and of the largest Lyapunov exponent when varying the parameters B and ν of the external forcing are presented in Fig. 3. Here, the basic state is taken to be the defect turbulence regime with $\alpha = -2$ and $\beta = 2$. Another representation of the results is used in Fig. 4 showing the contour lines for the nearly zero values of Ω , of the density of defects, and of the largest Lyapunov exponent.

According to these figures, we can distinguish four typical regimes when increasing the forcing amplitude B :

1. For small B , defect turbulence is only slightly disturbed, and no synchronization effects are detected.
2. Stronger forcing suppresses phase rotations, so that $\Omega = 0$, but the system remains turbulent. This is the region in Fig. 4 between the zero-level lines of Ω and of the Lyapunov exponent. We illustrate this regime of turbulent synchronization in Fig. 5. For larger forcing amplitudes B , no defects are observed (Fig. 5(a)), while near the border $\Omega = 0$ there are states where the averaged frequency is nearly zero, but for which some defects can still occur (dark spots in Fig. 5(b)). The contribution of these rare defects to the mean frequency is very small.
3. For relatively large forcing amplitudes, turbulence disappears and a regular (spatially and/or temporally periodic) synchronized state with zero largest Lyapunov exponent is observed.
4. For very large forcing amplitudes, the stable synchronized homogeneous solution with negative Lyapunov exponent (8) is observed (this state is not shown in Figs. 3 and 4 as it occurs for larger values of B).

4.2. Synchronizing phase turbulence

Phase turbulence is a weaker form of spatiotemporal chaos than most defect turbulence regimes (as seen, e.g., from the corresponding values of the largest Lyapunov exponents). It is thus expected to be easier to

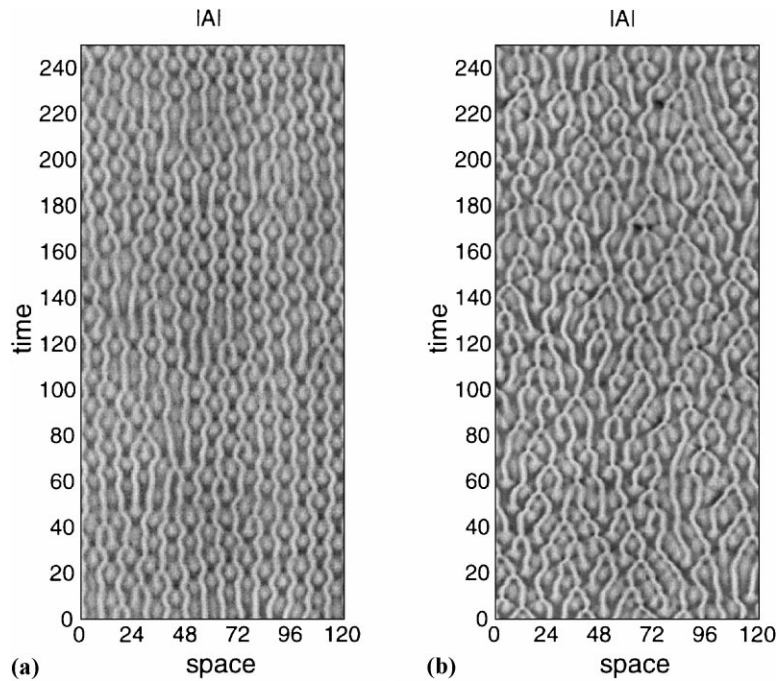


Fig. 5. Turbulent synchronization of defect turbulence $\beta = 2$, $\alpha = -2$. (a) In the region III of Fig. 4 ($\nu = -1.2$, $B = 0.35$), no defects are present. (b) In the region II of Fig. 4 ($\nu = -1.2$, $B = 0.23$), rare defects (dark spots) can be observed (e.g., at $x \approx 75$, $t \approx 225$); their contribution to the averaged frequency Ω is small.

synchronize, and this is confirmed by our numerical experiments. We have performed them for one particular set of parameters $\beta = 2$, $\alpha = -0.75$, so the results presented below do not represent the only possible scenario for the phase turbulence state.

Fig. 6 (a) shows the results of a parameter scan as in Fig. 3, measuring Ω , the density of defects, and the largest Lyapunov exponent for $\alpha = -0.75$ and $\beta = 2$. Here, the synchronization region is large and starts at small forcing amplitudes if the external frequency is in resonance with the frequency of natural rotations (note the difference in scales of Figs. 6(a) and 3). According to the calculations of the Lyapunov exponent (Fig. 6(c)), the synchronous state can be turbulent (positive exponent), periodic in space and/or in time (zero exponent), or constant and spatially homogeneous (negative exponent).

The rugged region at the border of the synchronization region in the frequency range $\nu < -0.76$ corresponds to the domain where there exists a finite space–time density of defects (Fig. 6(b)). The spatiotemporal

regimes in this region are illustrated in Fig. 7. Localized seagull-like structures arise from the defects and often lead to the creation of two new defects.

In the Section 5, we focus on these localized structures and show that they are related to 2π -phase kinks. We also characterize the state observed in Fig. 7 as a kink-breeding regime.

5. Phase kinks as natural excitations in the forced system

The spatially homogeneous static solution R_0, Φ_0 , when linearly stable, is not necessarily the global attractor of the system. Other stable solutions may exist. Intuitively, it is easy to understand that localized 2π -phase kinks are the natural candidates. Imagine an initial condition such that $R \approx R_0$ everywhere, but with large extremal deviations in the continuous phase profile. As the external forcing imposes a preferred value Φ_0 , the phase profile will develop steps at values such

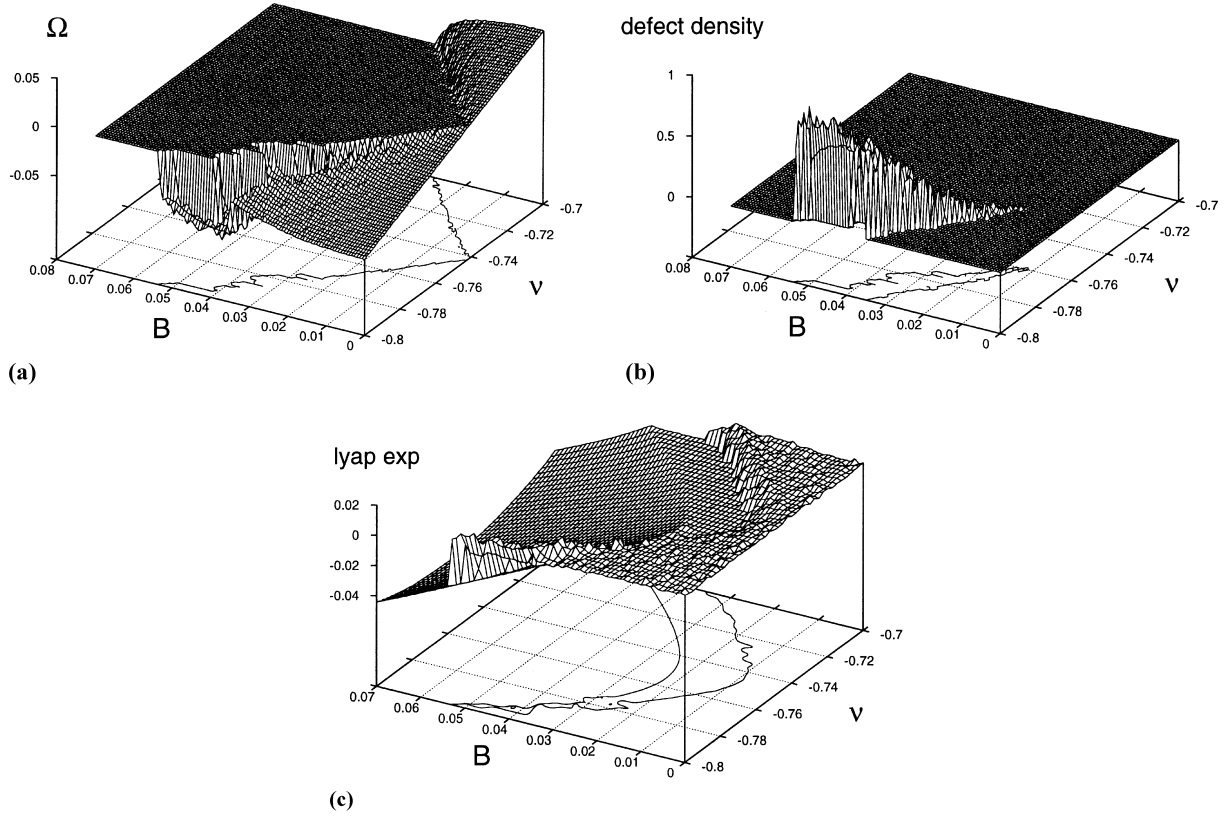


Fig. 6. Synchronization of phase turbulence. (a) The average frequency Ω as a function of the amplitude B and the frequency ν of the external force. The contour line shows the border of the synchronization region. (b) The density of defects (arbitrary units). (c) The largest Lyapunov exponent. The contour lines show the regions of positive, zero, and negative exponents.

that $\Phi = \Phi_0 \bmod 2\pi$. Given the local phase portrait (see Fig. 1), which “forbids” passing through the central focus, these steps are expected to be rather sharp: they should appear as 2π -phase kinks [22].

The isolated phase kink is a solitary wave propagating at constant speed (see Fig. 9(a)), whose profile is stationary in the frame moving at this velocity. It is thus natural to look for solutions satisfying the following ansatz:

$$A = R(\xi) \exp(\Phi(\xi)) \quad \text{with} \quad \xi = x - \nu t$$

with the constraints

$$\begin{aligned} R(\xi) &\rightarrow R_0 \quad \text{for} \quad \xi \rightarrow \pm\infty, \\ \Phi(\xi) &\rightarrow \Phi_0 \quad \text{for} \quad \xi \rightarrow -\infty, \\ \Phi(\xi) &\rightarrow \Phi_0 + 2\pi \quad \text{for} \quad \xi \rightarrow \infty. \end{aligned} \quad (13)$$

Substituting this ansatz in the forced CGLE leads to a boundary value problem in a four-dimensional ODE which is numerically rather complex to solve. Indeed, one has to find a homoclinic trajectory in the four-dimensional phase space that lies on the intersection of two-dimensional stable and unstable manifolds. The high dimension of the phase space and the absence of symmetry in the problem renders the application of a simple shooting algorithm hardly possible; the only hope may be in the implementation of recent advanced techniques [23,24].

The kink solution is, however, much easier to find within the phase approximation given by Eq. (6). Substituting $\Phi = \Phi(\xi)$, we get the second-order ODE

$$\begin{aligned} -V\Phi' &= \nu - \alpha - B \sin \Phi - \alpha B \cos \Phi \\ &+ (\alpha - \beta)(\Phi')^2 + (1 + \alpha\beta)\Phi'' \end{aligned} \quad (14)$$

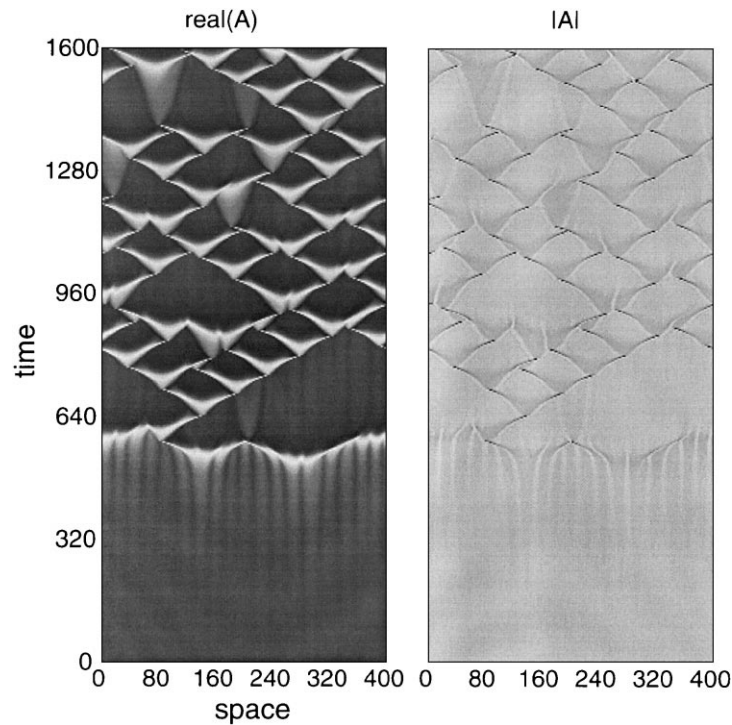


Fig. 7. Kink-breeding process in the phase turbulence for $\alpha = -0.75$, $\beta = 2$, $\nu = -0.8$, and $B = 0.041$. Initial conditions are small fluctuations around the unstable synchronized plane wave. Grey scale space–time plots of $\text{Re}(A)$ and $|A|$ reveal the occurrence of defects (black spots in the right panel) corresponding to zeros of $|A|$.

with boundary conditions (13). This problem can be easily solved numerically by matching stable and unstable one-dimensional manifolds of the fixed point. The matching condition determines the velocity V , and the kink profile can be obtained. We compare the solution of the phase equation with the phase kink obtained for the same parameters in the full forced CGLE in Fig. 8. Note that, in the $\alpha = \beta$ case, Eq. (14) coincides with the equation for stationary waves in the damped sine-Gordon equation [25].

The asymmetry of the kink can be seen as arising from the presence in the phase equation of the term Φ_x^2 , which breaks the $x \rightarrow -x$ symmetry for $\alpha \neq \beta$. Due to this asymmetry, the kink mainly propagates in one direction. The width of the kink is smaller on the left side of the Arnol'd tongue and its minimal amplitude is according to (5) smaller, too.

6. Complex dynamics of phase kinks

The direct study of the stability of the kink solution is a difficult problem made even more difficult in the absence, thus so far, of an explicit expression for this solution. In this section, we describe the results of numerical simulations in which a single kink is introduced into the various regimes of the CGLE.

Initial conditions consist of a localized 2π variation of the phase imposed on the homogeneous stationary solution (R_0, Φ_0) in a box with periodic boundary conditions.

6.1. Nonturbulent background

We have chosen the parameters $\beta = 0$ and $\alpha = 1$ for which no sustained disorder is observed in the CGLE. The synchronized spatially homogeneous state is then

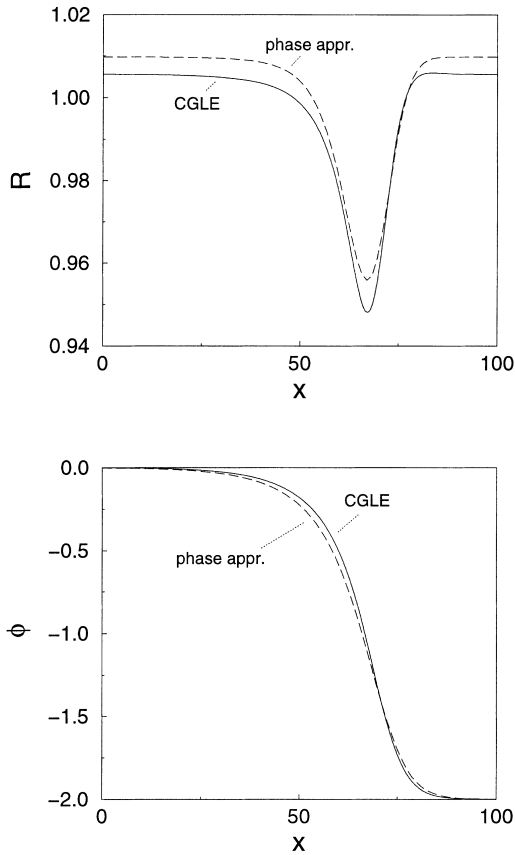


Fig. 8. The phase kink obtained as a solution of (14) and from the simulations of the full forced CGLE, for $\alpha = 0$, $\beta = 1$, $\nu = 0.995$, and $B = 0.02$.

stable in the whole Arnol'd tongue region. We have observed three different regimes of kink dynamics depending on the forcing parameters (see Fig. 9). The regions corresponding to these three regimes are not symmetric inside the Arnol'd tongue (cf. Fig. 6(b)).

1. *Stable stationary kink* (Fig. 9(a)): The initial profile evolves toward a stationary wave propagating with a constant velocity. For small forcing amplitudes, this kink is satisfactorily described by the phase equation (6).
2. *No kink solution* (Fig. 9(b)): The initial profile evolves to a rather narrow 2π -kink, which disappears via the creation of a defect – R vanishes at one point in space–time.
3. *Kink-breeding*: The initial kink disappears via the occurrence of a defect, but the residual perturba-

tion grows and leads to two new kinks. This is due to the excitability of the underlying system of ODEs (7) in this case: a finite perturbation to the homogeneous solution exceeds the threshold and leads to a 2π -shift of the phase. As the perturbation is local, two symmetric kinks are formed. The process then repeats itself: each of the new kinks dies and leads to the creation of two new kinks, etc. The asymptotic spatiotemporal evolution is a disordered state (see Fig. 9(c)). From the point of view of synchronization, this regime is characterized by the intermittent behavior of each site, which leads to the deviation of the mean frequency Ω from zero, as seen in Fig. 6(a).

6.2. Kinks and spatiotemporal intermittency

For the parameter values where spatiotemporal intermittency can be observed, the homogeneous plane wave solution is stable, and thus the phase kink is a stable localized excitation. Increasing the forcing amplitude B , the kink disappears via the occurrence of a defect, and this perturbation can trigger spatiotemporal intermittency regimes which resemble those observed without forcing (Fig. 10). One noticeable difference is that the phase within the large “laminar” regions tends to be close to Φ_0 . For very strong forcing, only the homogeneous synchronous state is observed.

6.3. Kinks and phase turbulence

We now return to the discussion of the kink-breeding state observed during the synchronization of phase turbulence (Section 4). The main difference with the kink-breeding regime described above is that here the disordered regime can set in even when starting from zero-winding number initial states of the CGLE, the phase turbulence fluctuations being strong enough to trigger it.

Decreasing the forcing amplitude, the homogeneous state (8) loses stability at the border given by Eq. (12), and spatially periodic stationary patterns appear. Correspondingly (Fig. 6(c)), the maximum Lyapunov exponent is zero in this region (because we consider the system with periodic boundary con-

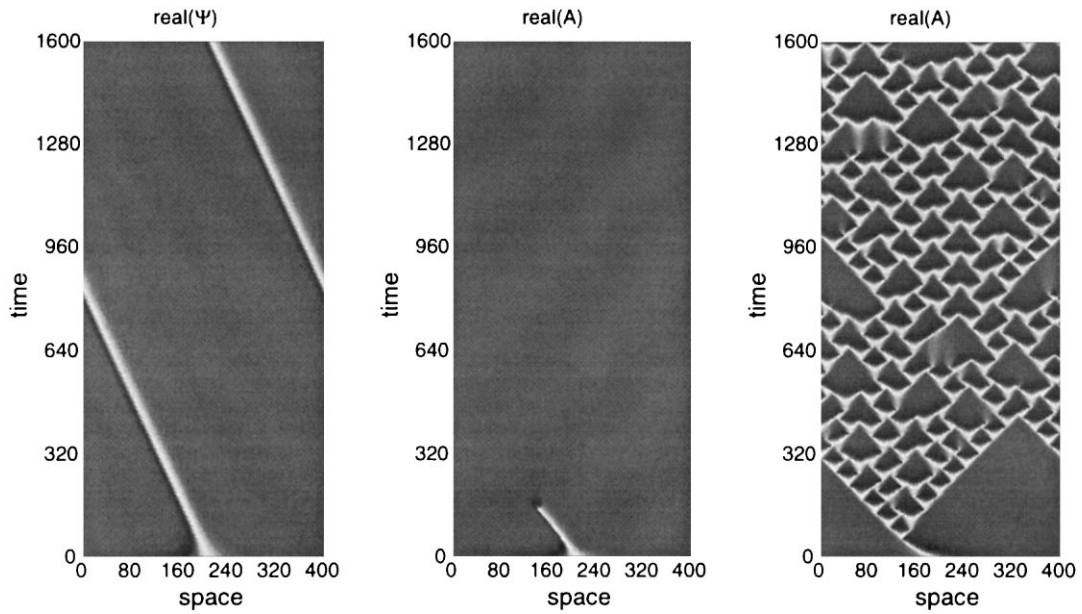


Fig. 9. Different regimes of kink dynamics for $\beta = 0$, $\alpha = 1$: (a) $\nu = 1$, $B = 0.02$; (b) $\nu = 1$, $B = 0.043$; (c) $\nu = 1.1$, $B = 0.073$.

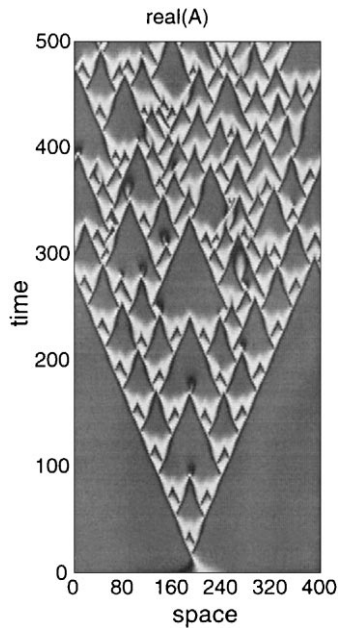


Fig. 10. Triggering of spatiotemporal intermittency from an initial kink for $\beta = 0$, $\alpha = 2$, $\nu = 2$, and $B = 0.08$.

ditions, spatial shifts of stationary nontrivial patterns are marginal and give rise to the zero Lyapunov exponent). Decreasing B further, one observes dif-

ferent regimes for different parts of the Arnol'd tongue.

1. On the right side of the Arnol'd tongue, i.e. for $\nu > \alpha$, we observe secondary instabilities of the periodic pattern. They are however soft and lead to a weakly turbulent regime which remains in the vicinity of the now unstable spatially homogeneous state. This state transits to phase turbulence as the forcing vanishes. Since no defects are observed for the whole range of B values, and since the amplitude is bounded away from zero, we can qualitatively interpret these transitions within the framework of the phase approximation. The external force in Eq. (6) provides a Φ -periodic potential which tends to bound the fluctuations of the phase. If the initial rotation number is zero, all the dynamics takes place in one valley of this potential, and the weakly chaotic state near the transition to turbulence is also bounded. One can say that the phase profile is “pinned” by the periodic potential. For smaller barrier heights, excursions of the phase to neighboring valleys are possible, and at some critical forcing amplitude, “depinning” occurs, leading to the onset of phase rotation and to the breakdown of synchronization.

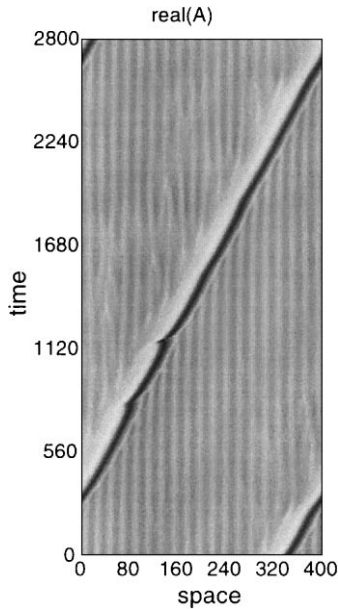


Fig. 11. Fluctuating kink on a turbulent background for $\beta = 2$, $\alpha = -0.75$, $\nu = -0.7$, and $B = 0.04$.

If a single 2π -phase rotation is imposed as an initial condition on the turbulent background, we can observe either the disappearance of the kink, or the conservation of the initial kink. In this latter case, the background remains turbulent, and the kink is not a perfectly stationary object in its moving frame: its velocity and its width fluctuate. Such a localized chaotic excitation is shown in Fig. 11.

- Another scenario is observed on the left side of the Arnol'd tongue, i.e., for $\nu < \alpha$. As the spatially periodic, stationary pattern develops, the spatial inhomogeneity leads to the spontaneous creation of phase kinks below a critical forcing (Fig. 7). The process of kink nucleation is similar to that of the regime of kink-breeding on a stable background: thanks to the excitability of the medium, a small local perturbation leads to a 2π -phase rotation from which two new kinks develop.

This stage can also be qualitatively described with the help of the phase approximation Eq. (6), combined with the ODE phase portrait of Fig. 1. Although the phase profile is mainly situated in-

side one valley of the potential, deviations from the stable state make it locally possible to visit the neighboring valley. As this happens for large potential barriers, the corresponding part of the phase profile slides to the bottom of the neighboring valley, and two relatively narrow kinks appear. The single phase kink is unstable in this region of parameters (so the two kinks disappear via defects, etc.), and the kink-breeding process sets in. It occupies a large region around the left border of the Arnol'd tongue (Fig. 6).

For very small forcing amplitudes, the barriers between potential valleys are small, the characteristic length of the kinks is large, and they are no more unstable. In fact, here one can hardly distinguish kinks from large-scale phase fluctuations, and the whole state continuously transits to phase turbulence as $B \rightarrow 0$.

7. Discussion and perspectives

In this paper, we considered the dynamics of the one-dimensional CGLE subject to periodic external forcing. At large forcing, complete synchronization is always achieved and the only stable solution is the spatially homogeneous state oscillating in synchrony with the forcing. For smaller forcing amplitudes, different partially synchronized states have been observed. We have argued that 2π -phase kinks are natural excitations in the forced system, which can be seen as mediating synchronization. In certain parameter regions, a kink-breeding process is observed, which destroys the perfect synchronization and is best described as a spatiotemporal intermittency regime, where synchronized regions are interrupted with phase slips. Moreover, when a phase turbulent state of CGLE is forced, kinks can appear spontaneously from the homogeneous state due to the combined effect of excitability and spatial instability.

We would like to emphasize that 2π -phase kinks are the natural consequence of the gauge invariance breaking combined with the excitability of the system. In this respect, they are different from the localized excitations observed in the normal CGLE (Nozaki-

Bekki holes [26,27], homoclinic holes [28]). Such kinks are natural for phase systems with broken gauge invariance like the sine-Gordon equation [29,30] or an analogous overdamped model studied recently [25]. In fact, the description of kinks in the framework of the phase equation is very close to that for the overdamped sine-Gordon model. The peculiar property of the forced CGLE model is that ... the amplitude is also present! Kinks are not topologically stable, they can appear and disappear through “defects”, i.e., points in space–time where the amplitude vanishes. This leads in particular to the nontrivial dynamics of kink-breeding.

The present work is only preliminary in that it does not provide a complete description of the various synchronization scenarios in the one-dimensional CGLE. Much remains to be done to assess the genericity of each route to and from complete synchronization. Similarly, we have not attempted here to systematically study the possible coexistence regions of the various dynamical phases discovered. This numerical exploration is left for future work, together with the determination of the kink solution, which should help in clarifying how the kink existence and stability regions influence the global synchronization properties of the medium.

Apart from a similar study in two space dimensions – a case of greater interest in an experimental context – specific problems have been located which deserve further investigations:

1. A systematic study of the influence of broken gauge invariance on the kinetic roughening properties of the phase interface of the forced CGLE. In the absence of defects, the phase of the medium can be seen as “pinned” (“synchronized”) at large forcing, and the subsequent depinning (desynchronization) transition observed when decreasing the forcing deserves attention.
2. the nature of the transition from kink-breeding to no-kink regimes: does this transition to spatiotemporal intermittency exhibit any critical region?

Acknowledgements

We thank M. Zaks, M. Rosenblum, J. Kurths, A. Mikhailov, A. Nepomnyashchy, and L. Pismen for valuable discussions. Support of the French–German Collaboration Program (PROCOPE) is acknowledged. This work was supported by ISI Foundation and EU HC&M Network ERB-CHRX-CT940546. AP acknowledges support of the Max-Planck-Society.

References

- [1] C. Hugueni, *Horologium Oscilatorium*, Paris, France, 1673.
- [2] I.I. Blekhman, *Synchronization in Science and Technology*, Nauka, Moscow, 1981 (in Russian); English transl.: ASME Press, New York, 1988.
- [3] P. Manneville, *Dissipative Structures and Weak Turbulence*, Academic Press, New York, 1989.
- [4] M.C. Cross, P.C. Hohenberg, *Rev. Mod. Phys.* 65 (1993) 851.
- [5] Y. Kuramoto, *Chemical Oscillations, Waves and Turbulence*, Springer, Berlin, 1984.
- [6] T. Leweke, M. Provansal, *Phys. Rev. Lett.* 72 (1994) 3174.
- [7] Q. Ouyang, J.-M. Flesselles, *Nature* 379 (1996) 6561.
- [8] B.I. Shraiman, A. Pumir, W. van Saarloos, P.C. Hohenberg, H. Chaté, M. Holen, *Physica D* 57 (1992) 241.
- [9] H. Chaté, *Nonlinearity* 7 (1994) 185.
- [10] H. Chaté, P. Manneville, *Physica A* 224 (1996) 348.
- [11] P. Manneville, H. Chaté, *Physica D* 96 (1996) 30.
- [12] I. Aranson, L. Aranson, L. Kramer, *Phys. Rev. A* 96 (1992) R2992.
- [13] I. Aranson, L. Kramer, A. Weber, *Phys. Rev. Lett.* 72 (1994) 2316.
- [14] W. van Saarloos, G. Huber, in: P.E. Cladis, P. Palffy-Muhoray (Eds.), *Spatiotemporal Patterns in Nonequilibrium Systems*, Addison-Wesley, Reading, MA, 1994.
- [15] P. Couillet, K. Emilsson, *Physica D* 61 (1992) 119.
- [16] P. Couillet, K. Emilsson, *Physica A* 188 (1992) 190.
- [17] D. Battogtokh, A. Mikhailov, *Physica D* 90 (1996) 84.
- [18] P. Glendinning, M. Proctor, *Int. J. Bifurcation and Chaos* 3 (1993) 1447.
- [19] O. Rudzick, Ph.D. Thesis, Universität Potsdam, 1998.
- [20] A.S. Pikovsky, *Sov. J. Commun. Technol. Electron.* 30 (1985) 85.
- [21] A. Pikovsky, M. Rosenblum, G. Osipov, J. Kurths, *Physica D* 104 (1997) 219.
- [22] B.A. Malomed, A.A. Nepomnyashchy, *Europhys. Lett.* 27 (1994) 649.
- [23] A.R. Champneys, Y.A. Kuznetsov, *Int. J. Bifurcation and Chaos* 4 (1994) 785.
- [24] A.R. Champneys, Y.A. Kuznetsov, B. Sandstede, *Int. J. Bifurcation and Chaos* 6 (1996) 867.

- [25] M. Argentina, P. Coulet, M. Mahadevan, *Phys. Rev. Lett.* 79 (1997) 2803.
- [26] K. Nozaki, N. Bekki, *J. Phys. Soc. Japan* 53 (1984) 1581.
- [27] K. Nozaki, N. Bekki, *Phys. Lett. A* 110 (1985) 133.
- [28] M. van Hecke, *Phys. Rev. Lett.* 80 (1998) 1896.
- [29] R. Dodd, J. Eilbeck, J. Gibbon, H. Morris, *Solitons and Nonlinear Wave Equations*, Academic Press, London, 1982.
- [30] A.C. Newell, *Solitons in Mathematics and Physics*, SIAM, Philadelphia, PA, 1985.